

## Article

# Enhanced Fe(III)/Fe(II) Redox Cycle for Persulfate Activation by Reducing Sulfur Species

Fujian Yang<sup>1,†</sup>, Cheng Yin<sup>2,†</sup>, Mengqiao Zhang<sup>1</sup>, Jiangwei Zhu<sup>3</sup>, Xiuyuan Ai<sup>1</sup>, Wenchao Shi<sup>1,\*</sup> and Guilong Peng<sup>1,\*</sup> 

<sup>1</sup> State Key Laboratory of Silkworm Genome Biology, Key Laboratory of Sericultural Biology and Genetic Breeding, Ministry of Agriculture and Rural Affairs, College of Sericulture, Textile and Biomass Sciences, Southwest University, Chongqing 400715, China

<sup>2</sup> Chongqing Monitoring Station, Water Quality Monitoring Network of National Urban Water Supply, Chongqing 400060, China

<sup>3</sup> Co-Innovation Center for Sustainable Forestry in Southern China, Nanjing Forestry University, Nanjing 210037, China

\* Correspondence: shiwenchaoyes@126.com (W.S.); pengguilong@swu.edu.cn (G.P.)

† These authors contribute equally to this work.

**Abstract:** The activation of persulfate (PS) by Fe(III) for the removal of environmental organic pollutants was severely limited by the low reduction rate from Fe(III) to Fe(II). In present study, we reported that reducing sulfur species (i.e.,  $\text{SO}_3^{2-}$ ,  $\text{HSO}_3^-$ ,  $\text{S}^{2-}$ , and  $\text{HS}^-$ ) under low concentration could significantly accelerate the Fe(III)/Fe(II) cycle in the Fe(III)/PS system. Under the condition of 1.0 mM Fe(III) and 4.0 mM PS, the removal performance of Fe(III)/PS system was poor, and only 21.6% of BPA was removed within 40 min. However, the degradation efficiency of BPA increased to 66.0%, 65.5%, 72.9% and 82.7% with the addition of 1.0 mM  $\text{SO}_3^{2-}$ ,  $\text{HSO}_3^-$ ,  $\text{S}^{2-}$ , and  $\text{HS}^-$ , respectively. The degradation efficiency of BPA was highly dependent on solution pH and the concentration of reducing sulfur species. When the reductant was excessive, the removal efficiency would be significantly inhibited due to the elimination of reactive species. This study provided some valuable insights for the treatment of organic wastewater containing these inorganic reducing ions.

**Keywords:** persulfate; reducing sulfur species; cycle; degradation



**Citation:** Yang, F.; Yin, C.; Zhang, M.; Zhu, J.; Ai, X.; Shi, W.; Peng, G. Enhanced Fe(III)/Fe(II) Redox Cycle for Persulfate Activation by Reducing Sulfur Species. *Catalysts* **2022**, *12*, 1435. <https://doi.org/10.3390/catal12111435>

Academic Editors: Jiangkun Du, Lie Yang and Chengdu Qi

Received: 30 September 2022

Accepted: 7 November 2022

Published: 15 November 2022

**Publisher's Note:** MDPI stays neutral with regard to jurisdictional claims in published maps and institutional affiliations.



**Copyright:** © 2022 by the authors. Licensee MDPI, Basel, Switzerland. This article is an open access article distributed under the terms and conditions of the Creative Commons Attribution (CC BY) license (<https://creativecommons.org/licenses/by/4.0/>).

## 1. Introduction

Advanced oxidation processes (AOP), usually including Fenton oxidation, persulfate oxidation, photocatalytic oxidation, electrochemical oxidation, chlorine oxidation, ozone oxidation etc [1–4]. Among them, iron-based peroxide activation process, including  $\text{H}_2\text{O}_2$  and persulfate (PS), have attracted extensive investigation interests because of their excellent performance and environmental friendliness. Similar to the traditional Fenton process, Fe(II) is one of the most commonly used PS activators to produce effective reactive oxidant species (ROS) [5]. However, the slow reduction rate from Fe(III) to Fe(II) seriously limited the application of Fe(III)/PS systems in the removal of environmental pollutants [6]. Thus, in recent years, Fe(II) regeneration in iron-based catalysts/PS systems has attracted more and more attention [7–9].

Interestingly, a large number of studies have confirmed that the use of reducing agents can significantly accelerate the Fe(III)/Fe(II) cycle and enhance the removal of organic pollutants during the activation of Fenton and iron-based persulfate [10–12]. However, the use of reducing agents in the iron-based persulfate reaction system will also lead to inevitable quenching effects of reactive species. Therefore, the use of reducing agents in the peroxide activation processes is actually a trade-off between the generation of reactive species and the elimination of reactive species [13]. Thus, it is of great importance to clarify the influence of above factors to control the production and elimination of reactive species.

Reductant and iron chelator are commonly used promoters of Fe(III) reduction. Reductants such as hydroxylamine [10,11,14], ascorbic acid [15,16], thiosulfate [17], and cysteine [18] can directly reduce Fe(III) to Fe(II), which is conducive to the reaction between Fe(II) and PS. To increase the concentration of dissolved iron species and regulating the redox potential of iron chelator complexes to accelerate the cycle of Fe(III)/Fe(II), iron chelating agents including citric acid [19], ethylenediaminetetraacetate (EDTA) [20] and ethylene diamine disuccinic acid (EDDS) [21] have been introduced into the system to enhance the degradation of organic pollutants. Meanwhile, many organic substances, such as gallic acid, hydroquinone, epigallocatechin-3-gallate and benzoquinone, can also provide electrons to Fe(III) through electron rich groups or their degradation by-products, which promotes the Fe(III)/Fe(II) cycle systems [22]. Although the addition of reducing agents can promote the regeneration of Fe(II) and improve the activation performance of PS, it may also lead to secondary pollution risk or increase the total organic carbon of the reaction system [12].

In view of the above problem, using reducing agents originally existing in the water to regenerate Fe(II) may be a good idea to improve PS activation efficiency and reduce external pollution. Sulfite and sulfide, as common inorganic reducing agent, widely exist in various industrial wastewaters, such as food processing, petroleum refining, tanneries, paper, and pulp manufacturing wastewater [22,23]. In consideration of the fact that sulfite and sulfide may be easy to obtain, and there are also many organic pollutants in these wastewaters, it is very important to look for S(IV)( $\text{SO}_3^{2-}$  / or  $\text{HSO}_3^-$ ) and S(-II)( $\text{S}^{2-}$  / or  $\text{HS}^-$ ) inorganic anions to promote the Fe(III)/Fe(II) cycle in the iron-based AOP and enhance the removal of organic pollutants in the wastewater. Because Fe(III) can oxidize S(IV)( $\text{SO}_3^{2-}$  /  $\text{HSO}_3^-$ ) to  $\text{SO}_4^{2-}$  [24], and S(-II)( $\text{S}^{2-}$  / or  $\text{HS}^-$ ) to  $\text{S}^0$  [22], interestingly, in this process, Fe(III) is also reduced to Fe(II), which may be an attractive strategy to promote the Fe(III)/Fe(II) cycle in AOPs.

Therefore, the main purpose of this study was to evaluate the effects of S(IV) and S(-II) on the activation performance in the PS/Fe(III) system. Bisphenol A (BPA), typical environmental hormone, usually used as a chemical material in various industries [25] and widely distributed in the water environment, was selected as the representative pollutant to investigate the effect of S(IV) and S(-II) on the activation efficiency of PS in the Fe(III)/PS process. Various parameters affecting the degradation efficiency of BPA were also investigated, including S(IV) and S(-II) dose, PS dose and pH value. This study will contribute to the construction of S(IV)/Fe(III)/PS and S(-II)/Fe(III)/PS systems, and provide some valuable insights for the treatment of organic wastewater containing these inorganic reducing ions.

## 2. Materials and Methods

### 2.1. Chemicals and Materials

The chemicals used in the experiments, including  $\text{Na}_2\text{S}\cdot 9\text{H}_2\text{O}$ , NaHS,  $\text{Na}_2\text{SO}_3$ ,  $\text{Na}_2\text{HSO}_3$ ,  $\text{FeSO}_4\cdot 7\text{H}_2\text{O}$ ,  $\text{FeNO}_3\cdot 9\text{H}_2\text{O}$ , NaCl,  $\text{Na}_2\text{S}_2\text{O}_8$  (PS), BPA, 1,10-phenanthroline, NaOH,  $\text{H}_2\text{SO}_4$ , and glacial acetic acid (HAc), were all purchased from Sinopharm Chemical Reagent Co., Ltd. (Shanghai, China). Methyl phenyl sulfoxide (PMSO) and methyl phenyl sulfone (PMSO<sub>2</sub>) were purchased from Macklin Biotechnology Co., Ltd. (Shanghai, China). Methanol (MeOH), ethanol (EtOH) and tert-butanol (TBA) were supplied by Aladdin Ltd. (Shanghai, China). Unless otherwise specified, all chemicals used were of analytical grade without further purification. All solutions were prepared with ultrapure water (resistance > 18.2 MΩ) from the Millipore Milli-Q water system.

### 2.2. Experimental Procedure

All experiments were performed in 150 mL conical flasks containing appropriate concentrations of BPA,  $\text{SO}_3^{2-}$  /  $\text{HSO}_3^-$  or ( $\text{S}^{2-}$  /  $\text{HS}^-$ ), PS and Fe(III), with a constant stirring rate at 25 °C, and the reaction was performed on the thermostat water bath. The pH of the reaction solutions was adjusted to the desired values with 0.1 M NaOH or  $\text{H}_2\text{SO}_4$ . 1.0 mL solution was withdrawn at predetermined time intervals, and quenched immediately

with 0.2 mL MeOH. Finally, the samples were filtered with 0.22- $\mu\text{m}$  PTFE membranes (Jinteng, China) before analysis with high performance liquid chromatography (HPLC). All experiments were conducted at least in duplicate, and the mean and average deviations were reported.

### 2.3. Analytical Methods

The concentration of BPA was analyzed on DIONEX UltiMate 3000 HPLC with a C-18 column (Agilent, 5  $\mu\text{m}$ , 250  $\times$  4.6 mm) and a UV detector. The mobile phase for the detection of BPA was consisted of 70% MeOH and 30% water (0.2% HAc) (*v/v*) at a flow rate of 1.0 mL  $\text{min}^{-1}$ , the retention time of BPA is 4.2 min. The column temperature and injection volume were set at 25  $^{\circ}\text{C}$  and 20  $\mu\text{L}$ , respectively. The concentration of regenerative Fe(II) was measured on HACH DR6000 UV-vis spectrophotometer by 1,10-Phenanthroline method [26]. The pH values of the solution were measured with a pH meter (FE28-Standard, Mettler Toledo, Greifensee, Switzerland).

## 3. Results and Discussion

### 3.1. Degradation Efficiency of BPA in Different Systems

In this study, the removal efficiencies of BPA in the Fe(III)/PS system with/without inorganic reducing ions were firstly conducted. As shown in Figure 1a, under the condition of 1.0 mM Fe(III) and 4.0 mM PS, the removal performance of Fe(III)/PS system was poor, and only 21.6% of BPA was removed within 40 min. This result might be attributed to the fact that Fe(III) can react with PS to regenerate Fe(II) through Equation (1) [27], the transformation of Fe(III) to Fe(II) is very limited, which is in accordance with the fact that Fe(III) cannot effectively activate PS [28]. When 1.0 mM S(IV) or S(-II) was added into the Fe(III)/PS system, the catalytic oxidation process was enhanced to various degrees. The degradation efficiency of BPA was 66.0%, 65.5%, 72.9% and 82.7% with the addition of 1.0 mM  $\text{SO}_3^{2-}$ ,  $\text{HSO}_3^-$ ,  $\text{S}^{2-}$ , and  $\text{HS}^-$ , respectively. These results indicated that the addition of inorganic reducing ions can remarkably improve the removal efficiency in the Fe(III)/PS system, which could be ascribed to the addition of inorganic reducing ions promoted the conversion of Fe(III) to Fe(II) via Equations (2)–(6) [29–32]. The inorganic reducing ions sulfur species could accelerate Fe(III)/Fe(II) cycle, and the regenerated Fe(II) significantly accelerated PS activation to enhance BPA degradation. Of note, the degradation of BPA in the Fe(II)/PS system was higher than that in the Fe(III)/PS system (Figure 1a), but lower than that of the Fe(III)/PS system incorporating inorganic reducing ions. These phenomena might be explained by the fact that both PS and the generated radicals could be consumed by the excessive Fe(II) [Equations (7)–(9)] [33,34], thus reducing the utilization efficiency of PS. In order to further confirm that this enhancement might be due to the S(IV) or S(-II) ions can promote the cycle of Fe(III)/Fe(II), accelerate the regeneration of Fe(II), and maintain high catalytic activity of the Fe(II)/PS system, the concentration of generated Fe(II) in S(IV) or S(-II)/Fe(III)/PS system was determined by 1,10-phenanthroline method [9] (Figure 1b). The concentrations of Fe(II) and Fe(III) were in a dynamic cycle within 40 min and remain relatively constant. The concentration of Fe(II) in the  $\text{S}^{2-}$ /Fe(III)/PS system was 0.89–0.96 mM, which was higher than that of the  $\text{HS}^-$ /Fe(III)/PS system (0.53–0.54 mM). The excess Fe(II) in the  $\text{S}^{2-}$ /Fe(III)/PS system might act as free radical scavenger, resulting in a lower removal of BPA than the  $\text{HS}^-$ /Fe(III)/PS system. The concentration changes of Fe(II) in the  $\text{SO}_3^{2-}$ /Fe(III)/PS and  $\text{HSO}_3^-$ /Fe(III)/PS system were comparable, which were 0.55–0.60 mM and 0.40–0.46 mM, respectively. Thus, no significant difference can be observed for the removal efficiency of BPA in the  $\text{SO}_3^{2-}$ /Fe(III)/PS and  $\text{HSO}_3^-$ /Fe(III)/PS systems. However, it was noted that the removal efficiencies of BPA (Figure 1a) were in the order of  $\text{HS}^-$ /Fe(III)/PS >  $\text{S}^{2-}$ /Fe(III)/PS >  $\text{SO}_3^{2-}$ /Fe(III)/PS >  $\text{HSO}_3^-$ /Fe(III)/PS > Fe(II)/PS > Fe(III)/PS, which were slightly different from the order of the concentration changes of Fe(II) in the Figure 1b ( $\text{S}^{2-}$ /Fe(III)/PS >  $\text{SO}_3^{2-}$ /Fe(III)/PS >  $\text{HS}^-$ /Fe(III)/PS >  $\text{HSO}_3^-$ /Fe(III)/PS) > Fe(II)/PS > Fe(III)/PS. On the one hand, in the presence of reducing sulfur species, the removal

efficiency of BPA can indeed be enhanced through the Fe(III)/Fe(II) redox cycle. On the other hand, in addition to the regeneration concentration of Fe(II), the removal efficiency of BPA may also be related to the chemical properties of reducing sulfur itself.

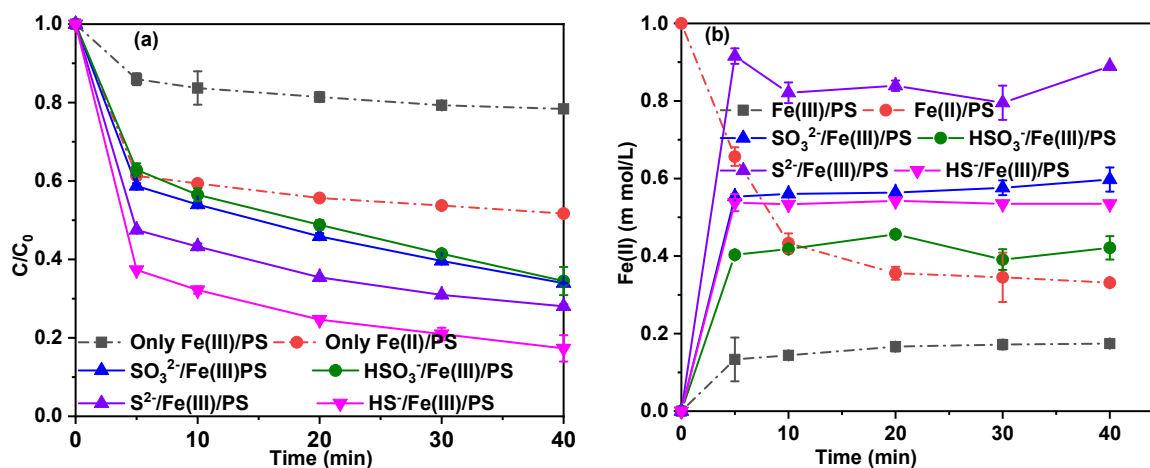
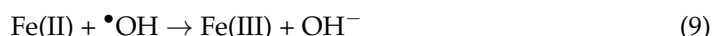
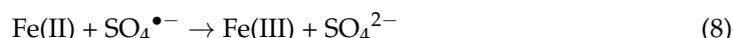
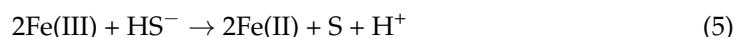
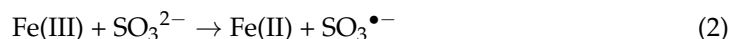


**Figure 1.** BPA removal in different systems (a); Concentration of regenerated Fe(II) in different systems (b). Reaction conditions: [Fe(III)] = 1.0 mM, [S(-II)] = [S(IV)] = 1.0 mM, [PS] = 4 mM, [BPA] = 10.0 mg/L.

In order to prove the dynamic cycle of Fe(II) and Fe(III), EDTA was used to compete for the Fe species with S species. Previous study have reported that Fe<sup>3+</sup>-EDTA complex was more stable than Fe<sup>2+</sup>-EDTA complex [35]. Figure S1 in the Supplementary Materials illustrates that BPA degradation efficiencies were dropped to 20.7%, 48.6%, 36.2%, and 32.6% in the SO<sub>3</sub><sup>2-</sup>/Fe(III)/PS, HSO<sub>3</sub><sup>-</sup>/Fe(III)/PS, S<sup>2-</sup>/Fe(III)/PS and HS<sup>-</sup>/Fe(III)/PS system, respectively. These results indicated that the addition of EDTA significantly inhibited the removal of BPA because the conversion between Fe(II) and Fe(III) is blocked, which further demonstrated the important roles of the dynamic cycle between Fe(II) and Fe(III).

### 3.2. Effect of SO<sub>3</sub><sup>2-</sup>/HSO<sub>3</sub><sup>-</sup>

Figure 2 and Table 1 show that BPA degradation efficiencies with initial concentrations of PS and Fe(III) increased from 25.1 to 82.7% and the rate constants increased remarkably from 0.0016 to 0.0216 min<sup>-1</sup> when the reducing sulfur species concentration increased from 0.1 to 1.0 mM. Meanwhile, the initial pH increased from 2.65 to 5.35 and the final pH increased from 2.51 to 3.23. As shown in Figure 2a, when the concentration of SO<sub>3</sub><sup>2-</sup> increased from 0.1 mM to 1.0 mM and 10.0 mM, the degradation efficiency of BPA increased from 25.1% to 66.0%, and then decreased to 2%, respectively, indicating that low concentration of SO<sub>3</sub><sup>2-</sup> could promote the degradation of BPA in the Fe(III)/PS system. Previous studies

have shown that the divalent and trivalent forms of iron exhibit reactivity in activating PMS and PS, but Fe(III) cannot activate the oxidants and generate ROS as effectively as Fe(II) [29]. Many researchers found that  $\text{SO}_3^{2-}$  could effectively promote the conversion from Fe(III) to Fe(II) according to Equation (2) [30]. The generated Fe(II) can catalyze persulfate to produce  $\text{SO}_4^{\bullet-}$  radicals as expressed by Equation (7) [33], which was conducive to the degradation of the BPA. However, when the concentration of  $\text{SO}_3^{2-}$  was further increased to 10.0 mM, the degradation reaction was nearly terminated, because the excess  $\text{SO}_3^{2-}$  would react with  $\text{SO}_4^{\bullet-}$  and  $\text{HO}^{\bullet}$  radicals according to Equations (10) and (11) [36].

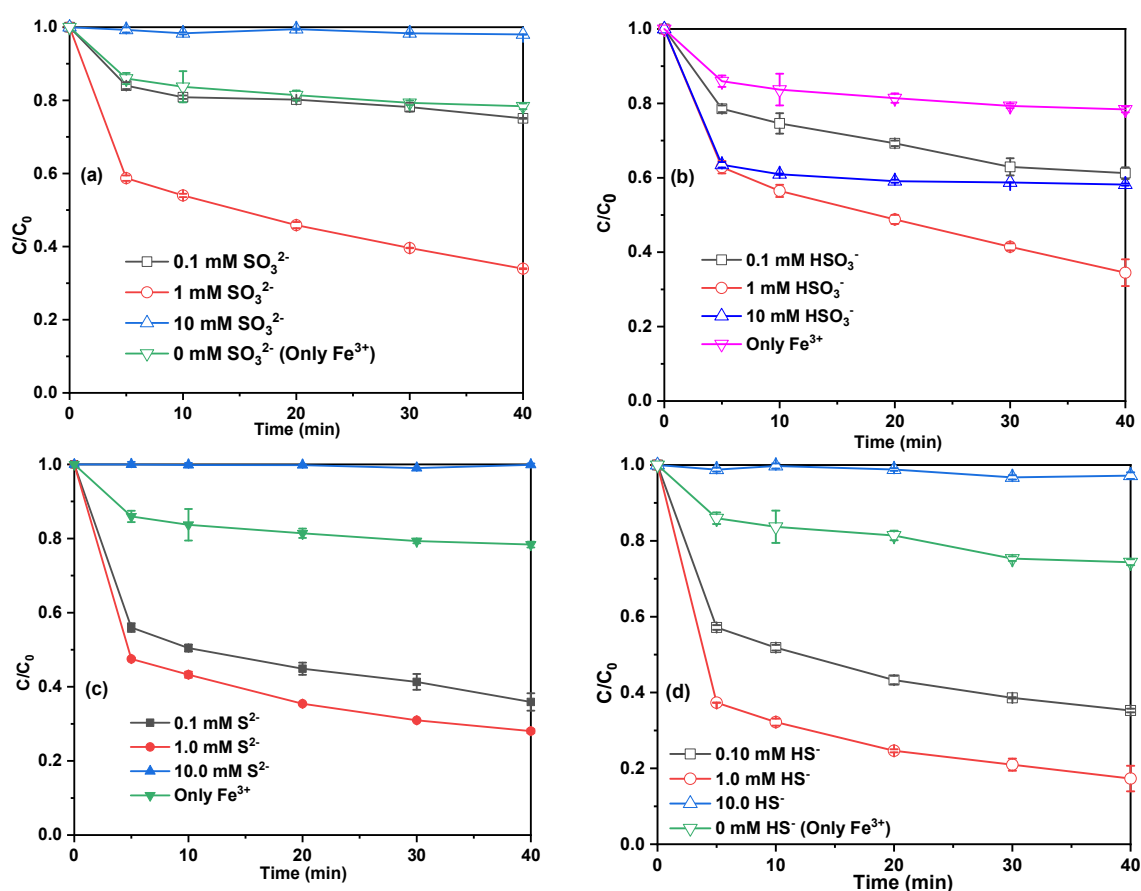
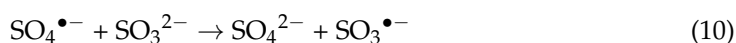
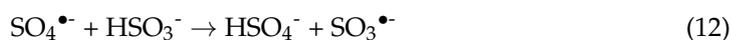


**Figure 2.** Effect of  $\text{SO}_3^{2-}$  (a);  $\text{HSO}_3^-$  (b);  $\text{S}^{2-}$  (c) and  $\text{HS}^-$  (d) on the removal efficiency of BPA. Reaction conditions:  $[\text{Fe(III)}] = 1.0 \text{ mM}$ ,  $[\text{PS}] = 4 \text{ mM}$ ,  $[\text{BPA}] = 10.0 \text{ mg/L}$ .

The degradation efficiency of BPA in the  $\text{HSO}_3^-/\text{Fe(III)}/\text{PS}$  system was described in Figure 2b, the degradation efficiency of BPA was 38.8%, 65.5% and 41.8% within 40 min with the addition of 0.1 mM, 1.0 mM and 10.0 mM of  $\text{HSO}_3^-$ , respectively. These results indicated that the degradation efficiency of BPA was enhanced when low concentrations of  $\text{HSO}_3^-$  ions were added in the Fe(III)/PS system, while high concentration  $\text{HSO}_3^-$  exhibited inhibitory effect on BPA removal. It might be attributed to Fe(III) being transformed to Fe(II) through Equations (3) and (4) [30], then PS is activated by Fe(II) ions to generate  $\text{SO}_4^{\bullet-}$  radicals, which was favorable for the degradation of BPA. However, high-concentration  $\text{HSO}_3^-$  disfavored the BPA removal due to excess  $\text{HSO}_3^-$  can act as scavenger to react with

$\text{SO}_4^{\bullet-}$  and  $\bullet\text{OH}$  (Equations (12) and (13)) [37,38], and produce  $\text{SO}_3^{\bullet-}$ ,  $\text{SO}_3^{\bullet-}$  with lower oxidation potential (0.63 V) [39], which cannot efficiently oxidize BPA.



### 3.3. Effect of $\text{S}^{2-}/\text{HS}^-$

As depicted in Figure 2c,d, the significant increased removal efficiency of BPA at the concentration of  $\text{S}^{2-}/\text{HS}^-$  0.1 mM and 1.0 mM would be obtained due to the S(-II) species have the ability to regenerate Fe(II) from Fe(III) via Equations (14) and (15) [31,32]. However, when the  $\text{S}^{2-}/\text{HS}^-$  concentration was increased to 10.0 mM, the removal of BPA could be ignored. This phenomenon could be attributed to the fact that PS can be consumed quickly by S(-II) via Equations (16) and (17) [40], and less generation of free radicals, which inhibited BPA degradation. In addition, excess  $\text{S}^{2-}/\text{HS}^-$  also could react with Fe(II) (Equations (18) and (19)) to produce FeS precipitation [31], which was not conducive to the activation of PS. For these reasons, when the  $\text{S}^{2-}/\text{HS}^-$  concentration was further increased to 10.0 mM, the degradation of BPA was significantly hampered.

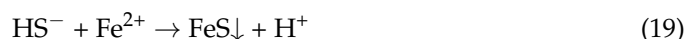
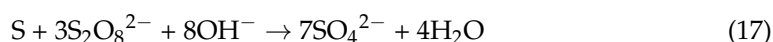
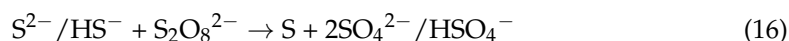
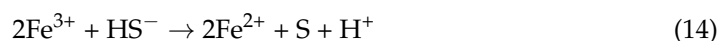


**Table 1.** The kinetics for BPA removal in 40 min under different S species ions conditions.

\	Removal (%)	$k_{obs}$ (min <sup>-1</sup> )	Half-Life ( $t_{1/2}$ , min)	Initial pH	Final pH
$\text{SO}_3^{2-}$ concentration (mM)					
0.1	25.1	0.0016	433.22	3.38	3.22
1.0	66.0	0.0155	44.72	5.35	3.23
10.0	2	/	/	8.01	7.80
$\text{HSO}_3^-$ concentration (mM)					
0.1	38.8	0.0062	111.80	2.81	2.75
1.0	65.5	0.0167	41.51	2.65	2.51
10.0	41.8	0.0022	315.07	2.44	2.27
$\text{S}^{2-}$ concentration (mM)					
0.1	64.1	0.012	57.76	3.19	3.11
1.0	71.9	0.0153	45.30	3.31	2.99
10.0	/	/	/	10.67	10.12
$\text{HS}^-$ concentration (mM)					
0.1	64.7	0.0138	50.23	2.93	2.91
1.0	82.7	0.0216	32.09	2.78	2.77
10.0	/	/	/	2.65	2.63

### 3.4. Influence of the Concentration of Fe(III)

The effects of different Fe(III) concentrations on the degradation of BPA were shown in Figure 3. The degradation efficiency of BPA increased from 6.2% to 70.1% and 45.8% to 73.2% for  $\text{SO}_3^{2-}/\text{Fe(III)}/\text{PS}$  and  $\text{HSO}_3^-/\text{Fe(III)}/\text{PS}$  system, 9.7% to 72.0% and 46.1% to 77.4% for  $\text{S}^{2-}/\text{Fe(III)}/\text{PS}$  and  $\text{HS}^-/\text{Fe(III)}/\text{PS}$  system, respectively, with the Fe(III) increasing from 0.1 mM to 1.0 mM. The possible reason was that an increase in Fe(III)

concentration resulted in more Fe(II) generation, which enhanced the activation of PS in S(IV)/Fe(III)/PS and S(-II)/Fe(III)/PS system.

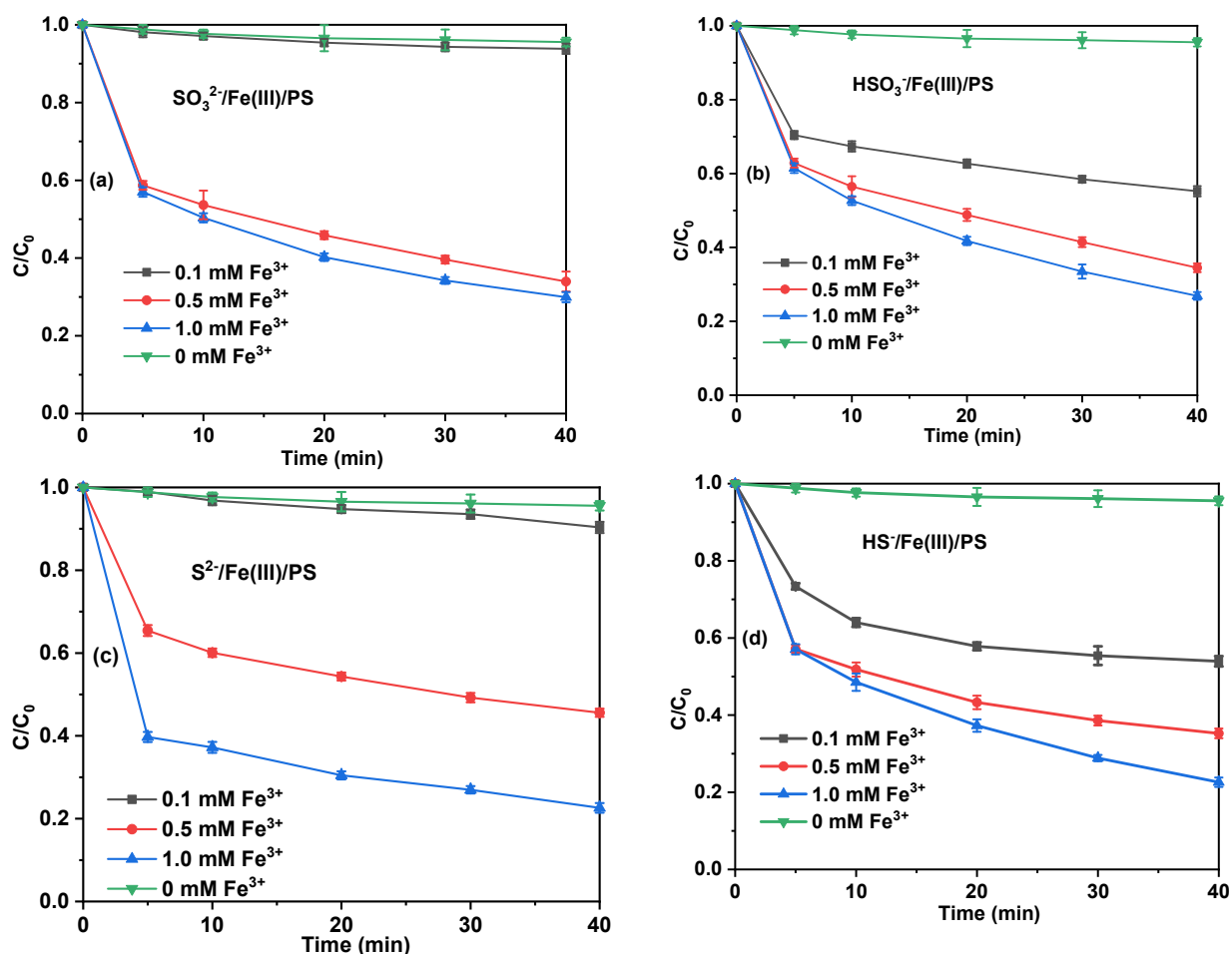


**Figure 3.** Effect of the concentration of Fe(III) on the removal efficiency of BPA in the  $SO_3^{2-}/Fe(III)/PS$  (a);  $HSO_3^-/Fe(III)/PS$  (b);  $S^{2-}/Fe(III)/PS$  (c) and  $HS^-/Fe(III)/PS$  (d) system. Reaction conditions:  $[SO_3^{2-}] = [HSO_3^-] = [S^{2-}] = [HS^-] = 1.0$  mM,  $[PS] = 4$  mM,  $[BPA] = 10.0$  mg/L.

### 3.5. Influence of Initial pH

As we know solution pH normally affects the form of iron. Thus, the effect of initial pH on BPA degradation in the S(IV)/Fe(III)/PS and S(-II)/Fe(III)/PS system was investigated in the absence of buffer, and the results are shown in Figure 4. Due to the strong acid ability of PS, the pH immediately dropped to 2.84 (as the control) when PS was introduced into the solution. Correspondingly, for the control experiments, the degradation efficiency of BPA was 70.1%, 73.2%, 72.0% and 77.4% in the  $SO_3^{2-}/Fe(III)/PS$ ,  $HSO_3^-/Fe(III)/PS$ ,  $S^{2-}/Fe(III)/PS$  and  $HS^-/Fe(III)/PS$  system, respectively. However, similar curves and performances of BPA degradation were obtained at pH 4.08 and 6.03, and significant inhibition of BPA degradation was observed when the initial pH of the solution was 4.08 and 6.03, which probably because Fe species are more readily precipitated in the form of oxyhydroxides at pH above 3.0 [34], and decrease the availability of Fe(II). These results indicated that the performance of S(IV)/Fe(III)/PS and S(-II)/Fe(III)/PS system are initial pH dependent. In addition, higher pH value (3–4) is more favorable for the formation of  $FeOH^+$  and  $Fe(OH)_2$ , and its activity is lower than  $Fe^{2+}$  [41], which is not conducive to the formation of  $SO_4^{\bullet-}$  and further BPA degradation [42].

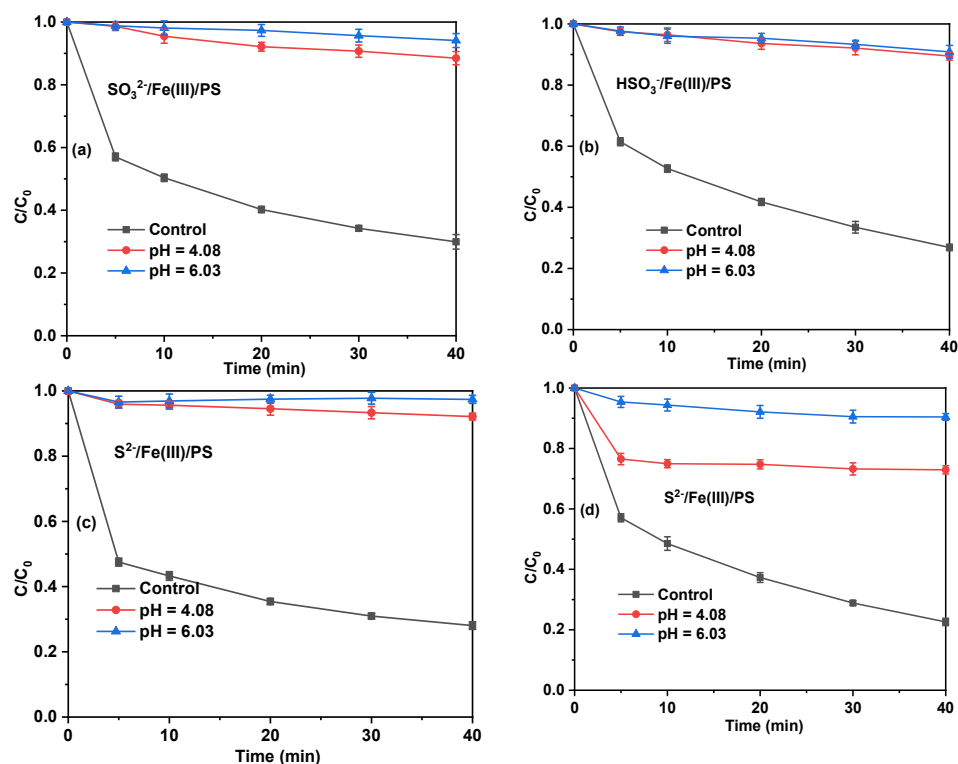


**Figure 4.** Effect of the initial pH on the removal efficiency of BPA in the  $\text{SO}_3^{2-}/\text{Fe(III)}/\text{PS}$  (a);  $\text{HSO}_3^-/\text{Fe(III)}/\text{PS}$  (b);  $\text{S}^{2-}/\text{Fe(III)}/\text{PS}$  (c) and  $\text{HS}^-/\text{Fe(III)}/\text{PS}$  (d) system. Reaction conditions:  $[\text{Fe(III)}] = 1.0 \text{ mM}$ ,  $[\text{SO}_3^{2-}] = [\text{HSO}_3^-] = [\text{S}^{2-}] = [\text{HS}^-] = 1.0 \text{ mM}$ ,  $[\text{PS}] = 4 \text{ mM}$ ,  $[\text{BPA}] = 10.0 \text{ mg/L}$ .

### 3.6. Identification of the Primary Reactive Oxidant Species

To elucidate the roles of radicals for BPA degradation in the  $\text{S(IV)}/\text{Fe(III)}/\text{PS}$  and  $\text{S(II)}/\text{Fe(III)}/\text{PS}$  system process, radical quenching experiments were conducted by using EtOH or TBA reagents. Due to the different kinetic constants, EtOH and TBA can be used to distinguish the contribution of  $\bullet\text{OH}$  and  $\text{SO}_4^{\bullet-}$  to the degradation of BPA in the reaction system [41]. The previous literature reported that EtOH could react with  $\bullet\text{OH}$  and  $\text{SO}_4^{\bullet-}$ , whereas TBA reacted with  $\bullet\text{OH}$  [5]. The effect of radical scavengers on the degradation of BPA is presented in Figure 5. The presence of EtOH shows a significant inhibitory effect on BPA removal, in the absence of scavengers, approximately 70.1%, 73.2%, 72.0% and 77.4% of BPA was degraded in the  $\text{SO}_3^{2-}/\text{Fe(III)}/\text{PS}$ ,  $\text{HSO}_3^-/\text{Fe(III)}/\text{PS}$ ,  $\text{S}^{2-}/\text{Fe(III)}/\text{PS}$  and  $\text{HS}^-/\text{Fe(III)}/\text{PS}$  system, respectively. However, when different concentrations of TBA or EtOH were added, the degradation of BPA showed different inhibition efficiency, which implied that  $\bullet\text{OH}$  and  $\text{SO}_4^{\bullet-}$  free radicals may be the main reaction species. With the addition of 0.1 and 1.0 M EtOH, the degradation efficiencies for BPA were dropped to 39.4% and 7.0%, 27.2% and 2.3%, 14.8% and 5.6%, and 16.4% and 7.5% in the  $\text{SO}_3^{2-}/\text{Fe(III)}/\text{PS}$ ,  $\text{HSO}_3^-/\text{Fe(III)}/\text{PS}$ ,  $\text{S}^{2-}/\text{Fe(III)}/\text{PS}$  and  $\text{HS}^-/\text{Fe(III)}/\text{PS}$  system, respectively. In addition, with the addition of 0.1 and 1.0 M TBA, the degradation efficiencies for BPA were dropped to 66.2% and 55.3%, 67.2% and 48.4%, 44.2% and 30.6%, and 52.2% and 12.2% in the  $\text{SO}_3^{2-}/\text{Fe(III)}/\text{PS}$ ,  $\text{HSO}_3^-/\text{Fe(III)}/\text{PS}$ ,  $\text{S}^{2-}/\text{Fe(III)}/\text{PS}$  and  $\text{HS}^-/\text{Fe(III)}/\text{PS}$  system, respectively. The difference in the quenching effects of EtOH and TBA was due to their different reactivity toward  $\text{SO}_4^{\bullet-}$  and  $\bullet\text{OH}$  [43]. The inhibition effect of EtOH was always stronger than TBA, especially when the concentration of EtOH increased to 1.0 M, the removal of BPA could be ignored. These results indicated that both  $\bullet\text{OH}$  and  $\text{SO}_4^{\bullet-}$  were present and responsible for the degradation of BPA, especially  $\text{SO}_4^{\bullet-}$  played a more critical role.

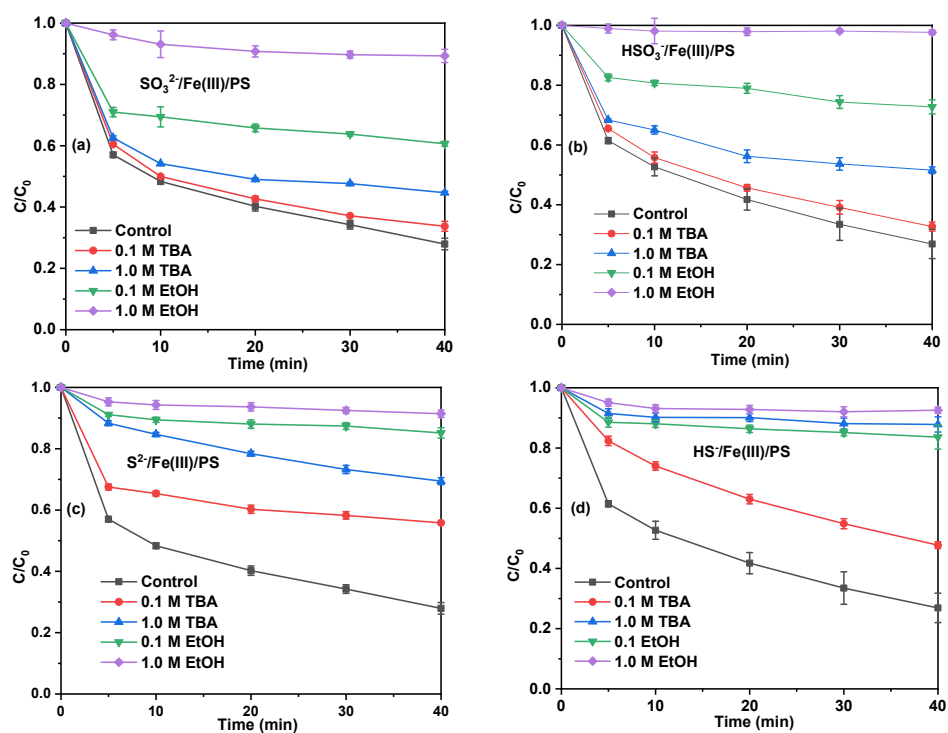
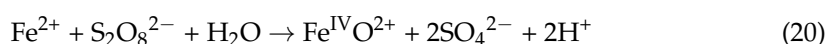


**Figure 5.** Effect of different quenchers on the removal efficiency of BPA in the  $\text{SO}_3^{2-}/\text{Fe(III)}/\text{PS}$  (a);  $\text{HSO}_3^-/\text{Fe(III)}/\text{PS}$  (b);  $\text{S}^{2-}/\text{Fe(III)}/\text{PS}$  (c) and  $\text{HS}^-/\text{Fe(III)}/\text{PS}$  (d) system. Reaction conditions:  $[\text{Fe(III)}] = 1.0 \text{ mM}$ ,  $[\text{SO}_3^{2-}] = [\text{HSO}_3^-] = [\text{S}^{2-}] = [\text{HS}^-] = 1.0 \text{ mM}$ ,  $[\text{PS}] = 4 \text{ mM}$ ,  $[\text{BPA}] = 10.0 \text{ mg/L}$ .

Recently, Wang et al. proposed that reactive species  $\text{Fe(IV)}$  was also formed in the  $\text{Fe(II)}/\text{PS}$  system (Equation (20)) [44]. Considering that  $\text{S(IV)}$  and  $\text{S(-II)}$  can reduce  $\text{Fe(III)}$  to  $\text{Fe(II)}$  and reconstruct the  $\text{Fe(II)}/\text{PS}$  system, to confirm whether  $\text{Fe(IV)}$  was generated in the  $\text{S(IV)}/\text{Fe(II)}/\text{PS}$  and  $\text{S(-II)}/\text{Fe(II)}/\text{PS}$  systems, PMSO was used as a probe compound because  $\text{Fe(IV)}$  can convert PMSO to  $\text{PMSO}_2$  [9,44], which was different from the radical-induced products. Figure S2a comparatively showed the degradation of PMSO (10 mg/L) in the  $\text{S(IV)}/\text{Fe(III)}/\text{PS}$  and  $\text{S(-II)}/\text{Fe(III)}/\text{PS}$  systems. As shown, the results indicated the extent of PMSO degradation was 73%, 79%, 78% and 87% in the  $\text{SO}_3^{2-}/\text{Fe(III)}/\text{PS}$ ,  $\text{HSO}_3^-/\text{Fe(III)}/\text{PS}$ ,  $\text{S}^{2-}/\text{Fe(III)}/\text{PS}$  and  $\text{HS}^-/\text{Fe(III)}/\text{PS}$  system, respectively. Meanwhile, 5.63, 7.56, 7.07 and 7.02 mg/L  $\text{PMSO}_2$  (Figure S2b) was formed in the  $\text{SO}_3^{2-}/\text{Fe(III)}/\text{PS}$ ,  $\text{HSO}_3^-/\text{Fe(III)}/\text{PS}$ ,  $\text{S}^{2-}/\text{Fe(III)}/\text{PS}$  and  $\text{HS}^-/\text{Fe(III)}/\text{PS}$  system, respectively. Furthermore, the yield of  $\text{PMSO}_2$  (i.e.,  $\eta(\text{PMSO}_2)$ , the molar ratio of  $\text{PMSO}_2$  generated to PMSO loss), was also quantified. As can be seen from Figure S2c,  $\eta(\text{PMSO}_2)$  value was 69.7%, 67.9%, 63.5% and 63.1% in the  $\text{SO}_3^{2-}/\text{Fe(III)}/\text{PS}$ ,  $\text{HSO}_3^-/\text{Fe(III)}/\text{PS}$ ,  $\text{S}^{2-}/\text{Fe(III)}/\text{PS}$  and  $\text{HS}^-/\text{Fe(III)}/\text{PS}$  system, respectively. The amount of generated  $\text{PMSO}_2$  was lower than the amount of degraded PMSO, which could be attributed to the fact that  $\text{Fe(IV)}$  was not the only reactive species causing the degradation of PMSO in this process. Because both  $\bullet\text{OH}$  and  $\text{SO}_4^{\bullet-}$  were reactive to PMSO but incapable of converting PMSO to  $\text{PMSO}_2$  [45].



#### 4. Conclusions

In the present study, we found that the presence of  $\text{SO}_3^{2-}/\text{HSO}_3^-$  and  $\text{S}^{2-}/\text{HS}^-$  can accelerate the  $\text{Fe(III)}/\text{Fe(II)}$  cycle in  $\text{PS}/\text{Fe(III)}$  system and improved the degradation efficiency of BPA, and good degradation efficiency can be obtained at medium acidity. In addition to  $\bullet\text{OH}$  and  $\text{SO}_4^{\bullet-}$ ,  $\text{Fe(IV)}$  was also involved in this process, and their contribution to the degradation of BPA was highly dependent on solution pH and the concentration of reducing sulfur species. The results indicated that both  $\text{S(IV)}$  (i.e.,  $\text{SO}_3^{2-}$  and  $\text{HSO}_3^-$ ) and

S(-II) (i.e.,  $S^{2-}$  and  $HS^-$ ) can reduce Fe(III) to Fe(II), and these reducing sulfur species were mainly responsible for enhancing Fe(III)/Fe(II) redox cycle, accelerating PS activation and pollutant degradation. With the addition of reductants, the removal efficiency of BPA would obviously accelerate. However, due to the quenching effect, the removal efficiency might decrease when the reductant was greatly excessive. This study can provide some valuable insights into the treatment of some organic wastewaters that contain  $SO_3^{2-}/HSO_3^-$  or  $S^{2-}/HS^-$ , and the results suggested that reducing agents have the great potential in breaking through the rate limit step and promoting the generation of reactive species. Furthermore, harmless and efficient reductants also should be encouraged to be explored for the application for peroxide activation.

**Supplementary Materials:** The following supporting information can be downloaded at: <https://www.mdpi.com/article/10.3390/catal12111435/s1>, Figure S1. Effect of EDTA on BPA removal in  $SO_3^{2-}/Fe(III)/PS$  and  $HSO_3^-/Fe(III)/PS$  systems (a) and  $S^{2-}/Fe(III)/PS$  and  $HS^-/Fe(III)/PS$  systems (b). Reaction conditions: [EDTA] = 1.0 mmol/L, [Fe(III)] = 1.0 mM, [S(-II)] = [S(IV)] = 1.0 mM, [PS] = 4 mM, [BPA] = 10.0 mg/L. Figure S2. PMSO depletion (a), PMSO<sub>2</sub> generation (b) and the yield of PMSO<sub>2</sub> (c). Reaction conditions: (a) PMSO: 10 mg/L, PS: 4 mmol/L, [Fe<sup>3+</sup>] = 1 mmol/L, [SO<sub>3</sub><sup>2-</sup>] = [HSO<sub>3</sub><sup>-</sup>] = [S<sup>2-</sup>] = [HS<sup>-</sup>] = 1 mmol/L and reaction time of 40 min.

**Author Contributions:** Study conception and design, all authors; experimental operation, F.Y., C.Y., M.Z., X.A. and W.S.; writing—review and editing, J.Z. and G.P.; funding acquisition—project, G.P. All authors have read and agreed to the published version of the manuscript.

**Funding:** This research received no external funding.

**Data Availability Statement:** All data, models, and code generated or used during the study appear in the submitted article.

**Acknowledgments:** This work was supported by the Natural Scientific Fund of Chongqing (no. cstc2020jcyj-msxmX0120), Graduate Education and Teaching Reform Research of Southwest University (no. SWUYJS226106), and the Central Universities (no. XDJK2019C045).

**Conflicts of Interest:** The authors declare no competing interest.

## References

1. Wang, X.; Chen, Z.; He, Y.; Yi, X.; Zhang, C.; Zhou, Q.; Xiang, X.; Gao, Y.; Huang, M. Activation of persulfate-based advanced oxidation processes by 1t-mos2 for the degradation of imidacloprid: Performance and mechanism. *Chem. Eng. J.* **2023**, *451*, 138575. [[CrossRef](#)]
2. Qi, C.; Yu, G.; Huang, J.; Wang, B.; Wang, Y.; Deng, S. Activation of persulfate by modified drinking water treatment residuals for sulfamethoxazole degradation. *Chem. Eng. J.* **2018**, *353*, 490–498. [[CrossRef](#)]
3. Qi, C.; Wen, Y.; Zhao, Y.; Dai, Y.; Li, Y.; Xu, C.; Yang, S.; He, H. Enhanced degradation of organic contaminants by fe(iii)/peroxymonosulfate process with l-cysteine. *Chin. Chem. Lett.* **2022**, *33*, 2125–2128. [[CrossRef](#)]
4. Dai, Y.; Qi, C.; Cao, H.; Wen, Y.; Zhao, Y.; Xu, C.; Yang, S.; He, H. Enhanced degradation of sulfamethoxazole by microwave-activated peracetic acid under alkaline condition: Influencing factors and mechanism. *Sep. Purif. Technol.* **2022**, *288*, 120716. [[CrossRef](#)]
5. Anipsitakis, G.P.; Dionysiou, D.D. Radical generation by the interaction of transition metals with common oxidants. *Environ. Sci. Technol.* **2004**, *38*, 3705–3712. [[CrossRef](#)]
6. Fan, J.; Gu, L.; Wu, D.; Liu, Z. Mackinawite (fes) activation of persulfate for the degradation of p-chloroaniline: Surface reaction mechanism and sulfur-mediated cycling of iron species. *Chem. Eng. J.* **2018**, *333*, 657–664. [[CrossRef](#)]
7. Zhang, Y.; Sun, J.; Guo, Z.; Zheng, X.; Guo, P.; Xu, J.; Lei, Y. The decomplexation of cu-edta by electro-assisted heterogeneous activation of persulfate via acceleration of fe(ii)/fe(iii) redox cycle on fe-mof catalyst. *Chem. Eng. J.* **2022**, *430*, 133025. [[CrossRef](#)]
8. Huang, M.; Wang, X.; Liu, C.; Fang, G.; Gao, J.; Wang, Y.; Zhou, D. Mechanism of metal sulfides accelerating fe(ii)/fe(iii) redox cycling to enhance pollutant degradation by persulfate: Metallic active sites vs. Reducing sulfur species. *J. Hazard. Mater.* **2021**, *404*, 124175. [[CrossRef](#)]
9. Liang, J.; Duan, X.; Xu, X.; Chen, K.; Wu, F.; Qiu, H.; Liu, C.; Wang, S.; Cao, X. Biomass-derived pyrolytic carbons accelerated fe(iii)/fe(ii) redox cycle for persulfate activation: Pyrolysis temperature-dependent performance and mechanisms. *Appl. Catal. B Environ.* **2021**, *297*, 120446. [[CrossRef](#)]
10. Chen, L.; Ma, J.; Li, X.; Zhang, J.; Fang, J.; Guan, Y.; Xie, P. Strong enhancement on fenton oxidation by addition of hydroxylamine to accelerate the ferric and ferrous iron cycles. *Environ. Sci. Technol.* **2011**, *45*, 3925–3930. [[CrossRef](#)]

11. Zou, J.; Ma, J.; Chen, L.; Li, X.; Guan, Y.; Xie, P.; Pan, C. Rapid acceleration of ferrous iron/peroxymonosulfate oxidation of organic pollutants by promoting fe(iii)/fe(ii) cycle with hydroxylamine. *Environ. Sci. Technol.* **2013**, *47*, 11685–11691. [[CrossRef](#)]
12. Zhou, H.; Peng, J.; Li, J.; You, J.; Lai, L.; Liu, R.; Ao, Z.; Yao, G.; Lai, B. Metal-free black-red phosphorus as an efficient heterogeneous reductant to boost fe<sup>3+</sup>/fe<sup>2+</sup> cycle for peroxymonosulfate activation. *Water Res.* **2021**, *188*, 116529. [[CrossRef](#)]
13. Zhou, H.; Zhang, H.; He, Y.; Huang, B.; Zhou, C.; Yao, G.; Lai, B. Critical review of reductant-enhanced peroxide activation processes: Trade-off between accelerated fe<sup>3+</sup>/fe<sup>2+</sup> cycle and quenching reactions. *Appl. Catal. B Environ.* **2021**, *286*, 119900. [[CrossRef](#)]
14. Hou, X.; Huang, X.; Jia, F.; Ai, Z.; Zhao, J.; Zhang, L. Hydroxylamine promoted goethite surface fenton degradation of organic pollutants. *Environ. Sci. Technol.* **2017**, *51*, 5118–5126. [[CrossRef](#)]
15. Hou, X.; Shen, W.; Huang, X.; Ai, Z.; Zhang, L. Ascorbic acid enhanced activation of oxygen by ferrous iron: A case of aerobic degradation of rhodamine b. *J. Hazard. Mater.* **2016**, *308*, 67–74. [[CrossRef](#)]
16. Sun, H.; Xie, G.; He, D.; Zhang, L. Ascorbic acid promoted magnetite fenton degradation ofalachlor: Mechanistic insights and kinetic modeling. *Appl. Catal. B Environ.* **2020**, *267*, 118383. [[CrossRef](#)]
17. Liang, C.; Bruell, C.J.; Marley, M.C.; Sperry, K.L. Persulfate oxidation for in situ remediation of tce. I. Activated by ferrous ion with and without a persulfate–thiosulfate redox couple. *Chemosphere* **2004**, *55*, 1213–1223. [[CrossRef](#)]
18. Li, T.; Zhao, Z.; Wang, Q.; Xie, P.; Ma, J. Strongly enhanced fenton degradation of organic pollutants by cysteine: An aliphatic amino acid accelerator outweighs hydroquinone analogues. *Water Res.* **2016**, *105*, 479–486. [[CrossRef](#)]
19. Wu, X.; Gu, X.; Lu, S.; Xu, M.; Zang, X.; Miao, Z.; Qiu, Z.; Sui, Q. Degradation of trichloroethylene in aqueous solution by persulfate activated with citric acid chelated ferrous ion. *Chem. Eng. J.* **2014**, *255*, 585–592. [[CrossRef](#)]
20. He, J.; Yang, X.; Men, B.; Yu, L.; Wang, D. Edta enhanced heterogeneous fenton oxidation of dimethyl phthalate catalyzed by fe<sub>3</sub>o<sub>4</sub>: Kinetics and interface mechanism. *J. Mol. Catal. A Chem.* **2015**, *408*, 179–188. [[CrossRef](#)]
21. Han, D.; Wan, J.; Ma, Y.; Wang, Y.; Li, Y.; Li, D.; Guan, Z. New insights into the role of organic chelating agents in fe(ii) activated persulfate processes. *Chem. Eng. J.* **2015**, *269*, 425–433. [[CrossRef](#)]
22. Hou, K.; Pi, Z.; Chen, F.; He, L.; Yao, F.; Chen, S.; Li, X.; Dong, H.; Yang, Q. Sulfide enhances the fe(ii)/fe(iii) cycle in fe(iii)-peroxymonosulfate system for rapid removal of organic contaminants: Treatment efficiency, kinetics and mechanism. *J. Hazard. Mater.* **2022**, *435*, 128970. [[CrossRef](#)]
23. Guerra-Rodríguez, S.; Cediél, N.; Rodríguez, E.; Rodríguez-Chueca, J. Photocatalytic activation of sulfite using fe(ii) and fe(iii) for enterococcus sp. Inactivation in urban wastewater. *Chem. Eng. J.* **2021**, *408*, 127326. [[CrossRef](#)]
24. Wang, Z.; Cao, L.; Wan, Y.; Wang, J.; Bai, F.; Xie, P. Enhanced degradation of tetrabromobisphenol a by fe<sup>3+</sup>/sulfite process under simulated sunlight irradiation. *Chemosphere* **2021**, *285*, 131442. [[CrossRef](#)] [[PubMed](#)]
25. Luo, H.; Lin, Q.; Zhang, X.; Huang, Z.; Fu, H.; Xiao, R.; Liu, S.-S. Determining the key factors of nonradical pathway in activation of persulfate by metal-biochar nanocomposites for bisphenol a degradation. *Chem. Eng. J.* **2020**, *391*, 123555. [[CrossRef](#)]
26. Harvey, A.E.; Smart, J.A.; Amis, E.S. Simultaneous spectrophotometric determination of iron(ii) and total iron with 1,10-phenanthroline. *Anal. Chem.* **1955**, *27*, 26–29. [[CrossRef](#)]
27. Wang, H.; Guo, W.; Yin, R.; Du, J.; Wu, Q.; Luo, H.; Liu, B.; Sseguya, F.; Ren, N. Biochar-induced fe(iii) reduction for persulfate activation in sulfamethoxazole degradation: Insight into the electron transfer, radical oxidation and degradation pathways. *Chem. Eng. J.* **2019**, *362*, 561–569. [[CrossRef](#)]
28. Liang, C.; Liang, C.-P.; Chen, C.-C. Ph dependence of persulfate activation by edta/fe(iii) for degradation of trichloroethylene. *J. Contam. Hydrol.* **2009**, *106*, 173–182. [[CrossRef](#)]
29. Xiao, S.; Cheng, M.; Zhong, H.; Liu, Z.; Liu, Y.; Yang, X.; Liang, Q. Iron-mediated activation of persulfate and peroxymonosulfate in both homogeneous and heterogeneous ways: A review. *Chem. Eng. J.* **2020**, *384*, 123265. [[CrossRef](#)]
30. Chen, Y.; Tong, Y.; Xue, Y.; Liu, Z.; Tang, M.; Huang, L.-Z.; Shao, S.; Fang, Z. Degradation of the β-blocker propranolol by sulfite activation using fes. *Chem. Eng. J.* **2020**, *385*, 123884. [[CrossRef](#)]
31. Ma, S.; Noble, A.; Butcher, D.; Trouwborst, R.E.; Luther, G.W. Removal of h<sub>2</sub>s via an iron catalytic cycle and iron sulfide precipitation in the water column of dead end tributaries. *Estuar. Coast. Shelf Sci.* **2006**, *70*, 461–472. [[CrossRef](#)]
32. Wu, G.; Kong, W.; Gao, Y.; Kong, Y.; Dai, Z.; Dan, H.; Shang, Y.; Wang, S.; Yin, F.; Yue, Q.; et al. Removal of chloramphenicol by sulfide-modified nanoscale zero-valent iron activated persulfate: Performance, salt resistance, and reaction mechanisms. *Chemosphere* **2022**, *286*, 131876. [[CrossRef](#)]
33. Xu, X.-R.; Li, X.-Z. Degradation of azo dye orange g in aqueous solutions by persulfate with ferrous ion. *Sep. Purif. Technol.* **2010**, *72*, 105–111. [[CrossRef](#)]
34. Li, X.; Ma, J.; Gao, Y.; Liu, X.; Wei, Y.; Liang, Z. Enhanced atrazine degradation in the fe(iii)/peroxymonosulfate system via accelerating fe(ii) regeneration by benzoquinone. *Chem. Eng. J.* **2022**, *427*, 131995. [[CrossRef](#)]
35. Jones, A.M.; Griffin, P.J.; Waite, T.D. Ferrous iron oxidation by molecular oxygen under acidic conditions: The effect of citrate, edta and fulvic acid. *Geochim. Cosmochim. Acta* **2015**, *160*, 117–131. [[CrossRef](#)]
36. Chen, Y.; Li, M.; Tong, Y.; Liu, Z.; Fang, L.; Wu, Y.; Fang, Z.; Wu, F.; Huang, L.-Z. Radical generation via sulfite activation on nife<sub>2</sub>o<sub>4</sub> surface for estriol removal: Performance and mechanistic studies. *Chem. Eng. J.* **2019**, *368*, 495–503. [[CrossRef](#)]
37. Buxton, G.V.; McGowan, S.; Salmon, G.A.; Williams, J.E.; Wood, N.D. A study of the spectra and reactivity of oxysulphur-radical anions involved in the chain oxidation of s(IV): A pulse and γ-radiolysis study. *Atmos. Environ.* **1996**, *30*, 2483–2493. [[CrossRef](#)]

38. Buxton, G.V.; Greenstock, C.L.; Helman, W.P.; Ross, A.B. Critical review of rate constants for reactions of hydrated electrons, hydrogen atoms and hydroxyl radicals ( $\cdot\text{oh}/\cdot\text{o}-$ ) in aqueous solution. *Phys. Chem. Ref. Data* **1988**, *17*, 513–886. [[CrossRef](#)]
39. Wu, S.; Shen, L.; Lin, Y.; Yin, K.; Yang, C. Sulfite-based advanced oxidation and reduction processes for water treatment. *Chem. Eng. J.* **2021**, *414*, 128872. [[CrossRef](#)]
40. Peng, J.; Lu, X.; Jiang, X.; Zhang, Y.; Chen, Q.; Lai, B.; Yao, G. Degradation of atrazine by persulfate activation with copper sulfide (cus): Kinetics study, degradation pathways and mechanism. *Chem. Eng. J.* **2018**, *354*, 740–752. [[CrossRef](#)]
41. Shi, X.; Li, Y.; Zhang, Z.; Sun, L.; Peng, Y. Enhancement of ciprofloxacin degradation in the fe(ii)/peroxymonosulfate system by protocatechuic acid over a wide initial ph range. *Chem. Eng. J.* **2019**, *372*, 1113–1121. [[CrossRef](#)]
42. Guo, J.; Gao, Q.; Yang, S.; Zheng, F.; Du, B.; Wen, S.; Wang, D. Degradation of pyrene in contaminated water and soil by fe<sup>2+</sup>-activated persulfate oxidation: Performance, kinetics, and background electrolytes (cl<sup>-</sup>, hco<sub>3</sub><sup>-</sup> and humic acid) effects. *Process Saf. Environ. Prot.* **2021**, *146*, 686–693. [[CrossRef](#)]
43. Yu, Y.; Li, S.; Peng, X.; Yang, S.; Zhu, Y.; Chen, L.; Wu, F.; Mailhot, G. Efficient oxidation of bisphenol a with oxysulfur radicals generated by iron-catalyzed autoxidation of sulfite at circumneutral ph under uv irradiation. *Environ. Chem. Lett.* **2016**, *14*, 527–532. [[CrossRef](#)]
44. Wang, Z.; Jiang, J.; Pang, S.; Zhou, Y.; Guan, C.; Gao, Y.; Li, J.; Yang, Y.; Qiu, W.; Jiang, C. Is sulfate radical really generated from peroxydisulfate activated by iron(ii) for environmental decontamination? *Environ. Sci. Technol.* **2018**, *52*, 11276–11284. [[CrossRef](#)]
45. Zong, Y.; Guan, X.; Xu, J.; Feng, Y.; Mao, Y.; Xu, L.; Chu, H.; Wu, D. Unraveling the overlooked involvement of high-valent cobalt-oxo species generated from the cobalt(ii)-activated peroxymonosulfate process. *Environ. Sci. Technol.* **2020**, *54*, 16231–16239. [[CrossRef](#)]